

PREDICTION MODEL OF AMMONIA CONCENTRATION IN YELLOW-FEATHER BROILERS HOUSE DURING WINTER BASED ON EEMD-GRU

基于 EEMD-GRU 的黄羽鸡舍冬季氨气浓度预测模型

Zeying Xu ¹⁾, Xiuguo Zou ^{*}, Zhengling Yin, Shikai Zhang, Yuanyuan Song, Jie Zhang, Jingxia Lu ¹

¹⁾ College of Engineering, Nanjing Agricultural University / China

Corresponding author: Xiuguo Zou

Tel: +862558606585; E-mail: xiuguozou@gmail.com

DOI: <https://doi.org/10.35633/inmateh-61-07>

Keywords: broiler house, ammonia concentration, winter, neural network

ABSTRACT

In winter, the poor ventilation conditions in broiler houses may lead to high ammonia concentration, which affects the health of yellow-feather broilers or even causes the death of many broilers. This research used a machine learning model to predict the ammonia concentration in a broiler house during winter. After analysis, it was found that the ammonia generation in the broiler house was a gradual accumulation featured by non-linear data. After the broilers entered the broiler house for several days, and the ammonia concentration reached a certain value, a ventilation system was used for regulating the concentration. Firstly, the back-propagation (BP) neural network model and gated recurrent unit (GRU) model were used for predicting the ammonia concentration, respectively. Then, ensemble empirical mode decomposition (EEMD) was performed on the time series data of ammonia concentration in the broiler house. After that, the EEMD-GRU prediction model has been established for the intrinsic mode function (IMF) components and the temperature and humidity data in the broiler house. Finally, all component results were summarized to obtain the final prediction result. A comparison was conducted among the prediction results obtained by the above three models. The results show that the root mean square errors of the above three models are 6.2 ppm, 4.4 ppm, and 2.4 ppm, respectively, and the average absolute errors were 4.9 ppm, 2.8 ppm, and 1.6 ppm, respectively. It could be seen that the EEMD-GRU model had higher accuracy in predicting the ammonia concentration in the broiler house. The EEMD-GRU model can effectively predict the ammonia concentration in broiler houses, facilitating the feedback to the central system for timely adjustment.

摘要

针对冬季鸡舍通风限制，舍内氨气浓度高，轻则影响黄羽鸡健康，重则导致大量鸡死亡的问题，本文采用机器学习模型对冬季黄羽鸡舍内的氨气浓度进行预测。分析发现鸡舍内氨气生成是一个逐渐累积的过程，数据具有非线性，在鸡只进入鸡舍氨气浓度达到一定值后，鸡舍内采用通风系统进行调控。本文首先选择 BP 神经网络模型和 GRU 模型进行预测，再对鸡舍氨气浓度时间序列数据进行集合经验模态分解，并分别对分解得到的 IMF 分量和鸡舍内对应时间的温度湿度数据建立 EEMD-GRU 预测模型，最后对每个分量结果求和得到最终的预测结果。通过三种模型的预测结果对比，得到预测结果的均方根误差分别为 6.2 ppm，4.4 ppm，2.4 ppm，平均绝对误差分别为 4.9 ppm，2.8 ppm，1.6 ppm。由此可见基于 EEMD-GRU 模型的鸡舍氨气浓度预测精度更高，更准确，在鸡舍中应用可以有效预测未来的氨气浓度，反馈给系统及时调控。

INTRODUCTION

As the living standards of the Chinese people are improving, the demand for meat consumption is also becoming diversified. This has accelerated the development of China's breeding industry. As the basic meat in people's lives, broiler meat deserves much attention from the breeding industry in terms of the quality and health of broilers. In broilers' breeding, environmental factors in broiler houses have important effects on the health and production of broilers, such as ammonia concentration. Ammonia is a colourless, poisonous gas with a strong pungent odour. The ammonia in a broiler house is mainly produced by the decomposition of broiler manure and nitrogen-containing organic matters.

¹Zeying Xu, Ms.; Xiuguo Zou, Assoc. Prof. Ph.D.; Zhengling Yin, Ms.; Shikai Zhang, MAE. Stud.;

Yuanyuan Song, MAE. Stud.; Jie Zhang, MAE. Stud.; Jingxia Lu, Assoc. Prof. Ph.D.

The high concentration of ammonia can not only affect the broiler's feed intake, feed conversion ratio (FCR) and productivity, but also cause damage to the broiler's respiratory system, which may reduce the quality of broiler (Yao Z., 2008). Therefore, it is of great significance to reasonably, timely, and accurately analyse and predict the ammonia concentration in broiler houses, so as to provide a reference for breeders to take corresponding measures.

Liu et al. (Liu W., 2019) implemented structural partitioning of a broiler house in Shandong Province along with horizontal and vertical directions. Based on the ammonia concentration data at each point monitored from 2014 to 2015, the single factor analysis method was used to obtain the daily ammonia concentration change in the broiler house and the ammonia gas distribution pattern between different cross-sections. They also proposed corresponding measures to reduce the ammonia concentration. Shen et al. (Shen D., 2018) used the statistical data of environmental indicators such as ammonia concentration detected in a broiler house to obtain the statistical characteristics of the distribution of air pollutants in the broiler house and the main sources of pollutants. Zilio et al. (Zilio M., 2020) determined the main contributor to the ammonia emissions of livestock farms using the seasonally sampled feces and ammonia data from four livestock farms in Italy from 2015 to 2017 through partial least squares (PLS) regression. They found that temperature was the main predictor of ammonia concentration. In summary, researchers have conducted extensive research on the poisonous gas emissions and distribution patterns in broiler houses. Multivariate statistical analysis and empirical models have played a very important role in the above research. However, the concentration data of various environmental factors in a broiler house are mostly non-stationary. This means that statistical methods cannot accurately predict the concentration of pollutants in a broiler house in a timely manner, and cannot provide a more accurate reference on breeding schemes for breeders.

With the development of artificial neural networks (ANN), traditional machine learning algorithms have been widely used in many research fields. Huo (Huo C., 2018) used a gray neural network algorithm and corrected the residual error through BP neural network to predict the ammonia concentration in a piggery, with a prediction accuracy of 94%. In the same year, Richardson et al. (Ribeiro R., 2019) established the ANN-Bayesian regularization model, and used the historical environment data of a broiler house to generate a set of parameters for the controller to make a correct response, which reduced the labour cost of poultry management. Xie (Xie Q., 2015) used the ANFIS-based algorithm to establish a model for ammonia concentration prediction in pig houses in different seasons, and analysed and obtained the correlation between ammonia concentration and various environmental factors in pig houses. The smallest relative error of the predicted ammonia concentration was 0.0858. This model provides a reliable reference for the control of the environment in a pig house.

Researchers have made considerable improvements to the structure of neural networks in recent years to improve the training effect of neural networks. Deep learning networks and the various learning frameworks they generate have gradually become popular and applied in various fields, especially on the research of air pollutant concentration. Guo et al. (Hao G., 2019) used a deep neural network to predict the concentrations of PM_{2.5} and PM₁₀ in Beijing, and proposed a prediction method of spatial conversion. They investigated the spatial correlation between air pollutants, which provided new ideas for air quality prediction models. Wei et al. (Xu W., 2011) developed a soft sensor for predicting the ammonia concentration at the outlet of a factory using BP neural network. They proposed an improved particle swarm algorithm to optimize the BP neural network model. Compared with the other two models, this model showed higher accuracy and better generalization ability. Due to the strong memory function and the ability to effectively process time-series data, the long short term memory (LSTM) network has been widely used in various practical problems, e.g., human action recognition (Majd M., 2019), water level prediction for nuclear reactor pressurizer (Zhang J., 2019), and short-term economic load forecasts (Muzaffar S., 2019), etc. The GRU model is a variant of the LSTM model, which is simpler in structure and can reduce the iteration time to a certain extent. GRU has also been used in sentiment classification (Pu M., 2019), and travel pattern recognition (Guo M., 2019), etc.

In previous research, we have used the computational fluid dynamics (CFD) method to establish a 3D model of the broiler house designed in this paper, which proved that the ventilation system of the broiler house met the requirements for cooling, ventilation and comfortable breeding (Zhang S., 2019). The proposed method of using an inverter to control the negative pressure fan has been accepted by some breeding bases, and has a good prospect for further application (Yao H., 2018). In terms of the research on the temperature inside a broiler house, we used the optimized least squares support vector machine model

based on the improved particle swarm optimization algorithm to predict the temperature in a broiler house. The average absolute error was 0.787 °C (Zhang X., 2019).

Based on the BP neural network and GRU model, this paper constructs an EEMD-GRU model to predict the ammonia concentration in the broiler house. The EEMD-GRU model effectively uses the historical time series data in the broiler house, considers the non-stationarity of the environmental data, and can determine the information forgotten and retained at each step according to the activation function. The results show that the EEMD-GRU model can improve the prediction accuracy and reduce the iteration time.

MATERIALS AND METHODS

Data Acquisition

In this experiment, the ammonia concentration of the yellow-feather broiler house located in Jinniuhu Street, Luhe District, Nanjing City, Jiangsu Province, China, was used as the research object. Environmental monitoring sensors were installed in the broiler house, and environmental data were collected in real-time every 1 min and transmitted through the RS485 serial network. The broiler house is 1.9 m wide and 2.9 m long. Fig. 1 shows the internal scene of the broiler house. The experiment had 45 broilers in the broiler house, and 50833 pieces of environmental data and broilers situation data from December 5, 2019 to January 12, 2020 were used as experimental data in this paper, including ammonia concentration, temperature, humidity, age of broilers and time for broilers to enter the broiler house. Because the ammonia concentration, temperature and humidity inside and outside the broiler house would not change greatly within 1 h, this research used the average of minutely data within 1 h as the hourly data. A model was established using experimental data to predict the ammonia concentration of the broiler house in the next hour. The increase of ammonia concentration in the broiler house was a gradual process, as the ammonia concentration would change with the growing days of the broilers and the environmental factors inside and outside the broiler house. Table 1 shows some of the data in this experiment. Table 2 exhibits the result of the statistical analysis.



Fig. 1 – Internal scene of the broiler house

Sensors, cameras, and wind speed inverters, etc. were installed in the experimental broiler house to detect the environmental data in real-time and take corresponding measures. The temperature and humidity sensors were purchased from Shandong Renke Measurement & Control Technology Co., Ltd., with an accuracy of ± 0.5 °C and $\pm 3\%$ RH, respectively, and with a resolution of 0.1 °C and 0.1% RH, respectively. The PM_{2.5} sensor was also purchased from this company with an accuracy of $\pm 10\%$. The ammonia concentration sensor was also purchased from this company with a resolution of 0.1 ppm (parts per million, 1 ppm = 1 ml/m³). The above sensors all had a dimension of 110 mm × 85 mm × 44 mm.

Table 1

Experimental data from December 15 to December 31, 2019

| Time | Ammonia concentration (ppm) | Outside temperature (°C) | Outside relative humidity (%) | Inside temperature (°C) | Inside relative humidity (%) | Age of broiler (day) | Time for broilers to enter the broiler house(hour) |
|------------------|-----------------------------|--------------------------|-------------------------------|-------------------------|------------------------------|----------------------|--|
| 2019-12-15 00:00 | 2.3 | 13.6 | 77.9 | 15.1 | 69.7 | 84 | 202 |
| 2019-12-15 01:00 | 2.2 | 14.4 | 78.1 | 14.8 | 70.6 | 84 | 203 |
| 2019-12-15 02:00 | 2.2 | 14.2 | 74.6 | 14.1 | 66.4 | 84 | 204 |
| 2019-12-15 03:00 | 2.2 | 13.9 | 73.6 | 13.7 | 65.8 | 84 | 205 |
| 2019-12-15 04:00 | 2.1 | 13.7 | 73.9 | 13.7 | 68.3 | 84 | 206 |
| ⋮ | ⋮ | ⋮ | ⋮ | ⋮ | ⋮ | ⋮ | ⋮ |
| 2019-12-31 06:00 | 29.6 | 0.4 | 65.4 | 3.9 | 66.6 | 100 | 592 |
| 2019-12-31 07:00 | 29.0 | 0.2 | 66.0 | 3.9 | 67.0 | 100 | 593 |
| 2019-12-31 08:00 | 28.1 | 1.9 | 67.3 | 4.9 | 65.9 | 100 | 594 |
| 2019-12-31 09:00 | 27.1 | 3.2 | 63.0 | 6.1 | 64.1 | 100 | 595 |
| 2019-12-31 10:00 | 25.3 | 3.8 | 62.0 | 7.0 | 61.5 | 100 | 596 |

Table 2

Statistical analysis of environmental data

| Parameter | Data volume | Mean value | Standard deviation | Maximum value | Minimum value |
|---------------------------|-------------|------------|--------------------|---------------|---------------|
| Ammonia | 883 | 15.5 | 12.5 | 50 | 0 |
| Outside temperature | 883 | 10.8 | 3.9 | 23.3 | 0.2 |
| Inside temperature | 883 | 12.7 | 3.2 | 23.2 | 3.8 |
| Outside relative humidity | 883 | 81.7 | 11.4 | 97.8 | 36.2 |
| Inside relative humidity | 883 | 76.0 | 9.3 | 90.1 | 40.7 |

Data Processing Methods

• Data Normalization

Data normalization is to make the eigenvalues of different dimensions on the data set comparable to a certain extent, and to eliminate the dimensional and order of magnitude differences between the eigenvalues. If there is a large difference in the value of features on a data set, the features with larger values often make a greater contribution to the model's results. Therefore, in order to improve the convergence speed and accuracy, the ammonia concentration, temperature and humidity values in this research need to be normalized.

The normalization method adopted in this paper is the min-max scaling method. All the values are concentrated to 0-1 according to

$$x^* = \frac{x - x_{min}}{x_{max} - x_{min}} \quad (1)$$

where x^* is the normalized data, x is the original data, x_{min} and x_{max} are the minimum and maximum values of the eigenvalues of the original data, respectively.

• Data Interpolation

In the experiment, the data is collected every 1 min, and data missing often occurs due to the failure of the data acquisition device. The data set is interpolated by summing and averaging the data of one hour before and after the missing time as the missing data to make the time series of the data set more complete.

Establishment of the Model

TensorFlow is a powerful open-source software library developed for deep neural networks (DNN). It supports all popular languages, such as Python, C ++, and Java, etc., with the ability to work on multiple platforms, and has good visualization of computing charts. Based on the TensorFlow framework, the following three models are established in this research for prediction.

• **BP Neural Network Model**

Back propagation (BP) neural network is a multilayer feedforward neural network using an error back-propagation algorithm and consists of an input layer, a hidden layer, and an output layer. The basic steps of a BP neural network are as follows:

(1) The k^{th} output value y of output layer neuron is calculated forward by:

$$y_k = f(\sum_{h=1}^q w_h \times b_h - \theta) \tag{2}$$

where w_h represents the weight matrix from the h^{th} neuron of the hidden layer to the output layer, θ represents the threshold of neurons in the output layer, b_h represents the output of the h^{th} neuron in the hidden layer. f represents the activation function.

$$b_h = f(\sum_{i=1}^d v_{iq} \times x_i - \theta_h) \tag{3}$$

where v_{iq} represents the weight matrix from the i^{th} neuron of input layer to hidden layer, x_i represents the input of the i^{th} neuron in the input layer, θ_h represents the threshold value of the h^{th} neuron in the hidden layer.

$$v_{iq} = [v_{i1} \ v_{i2} \ v_{i3} \dots \ v_{iq}] \tag{4}$$

where d represents the number of neurons in the input layer, q represents the number of neurons in the hidden layer. In this paper: $d = 14$.

Final output value y of output layer:

$$y = [y_1 \ y_2 \dots \ y_k \dots \ y_n] \tag{5}$$

where n is the number of forecast samples.

The structure of the BP neuron model is shown in Fig. 2.

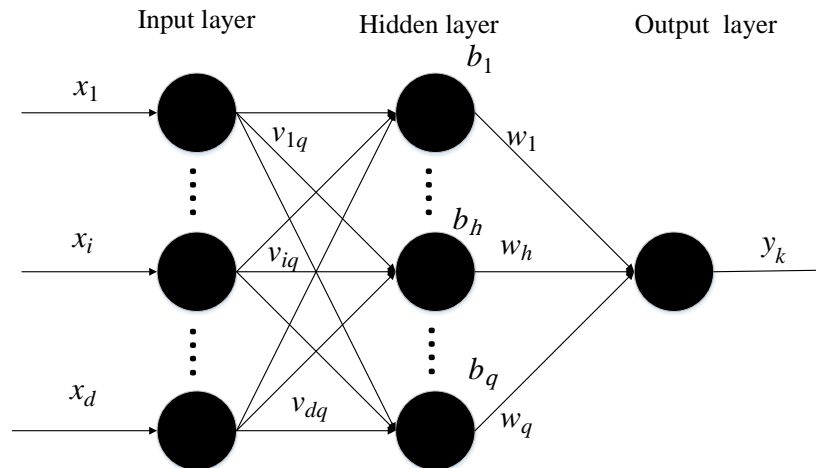


Fig. 2 – Structure diagram of BP neuron model

(2) If there is an error between the output value and the expected output value, the error term is back propagated.

$$E = \frac{1}{2} (y - y_r)^2 \tag{6}$$

where E represents the output error, y_r represents the expected output value.

(3) The gradient descent method is used to continuously iterate each neuron's weights to reduce the error term until it reaches the acceptable error range.

In this research, the ammonia concentration, temperature, and humidity of the broiler house in the previous two hours are used as input data. The ammonia concentration at the current moment is used as a label to construct a BP neural network sample.

The parameters of the BP model designed in this paper are shown in Table 3.

Table 3

| BP model's parameters | |
|--|---|
| Parameter | Parameter value |
| Training set | 70% of all data sets |
| Test set | 30% of all data sets |
| Optimizer | Adam adaptive moment estimation optimizer |
| Exponential decay rate of first-order moment estimation | 0.9 |
| Exponential decay rate of second-order moment estimation | 0.999 |
| Epsilon | 10^{-8} |
| Hide layer activation function | ReLU() |
| Number of Network layer | 3 |
| Number of hidden layer nodes | 10, 15 |
| Output layer activation function | ReLU() |
| Learning rate | 0.001 |

• GRU Model

The gated recurrent unit (GRU) model uses a recurrent neural network. The structure of the recurrent neural network is similar to that of a shallow neural network, which is composed of an input layer, a hidden layer, and an output layer. The difference is that the recurrent neural network is composed of multiple hidden layers, which deepens the depth of the network structure to a certain extent. The nodes in the hidden layer are connected to each other. When processing time-series data, the output result of each node is not only related to the current information input to the node, but also depends on the output result of the previous node, which means a function of memorizing. So, the recurrent neural networks are suitable for processing time series-data (Hu M., 2019). The LSTM recurrent neural network adds forget gate, input gate, and output gate to the original recurrent neural network structure. The opening and closing of these gates are determined by the activation function, which can determine whether the information of the upper layer is added to the calculation of this layer. However, its ability to learn complex long-sequence data is poor, and there will be the problems of gradient disappearance and gradient explosion during the learning process. The GRU model is a variant structural model of LSTM, but simpler in structure, which reduces the iteration time. There are only two gates in the GRU structure, namely, update gate and reset gate. The update gate can be seen as a combination of the forget gate and input gate in the LSTM model. The GRU network structure is shown in Fig. 3.

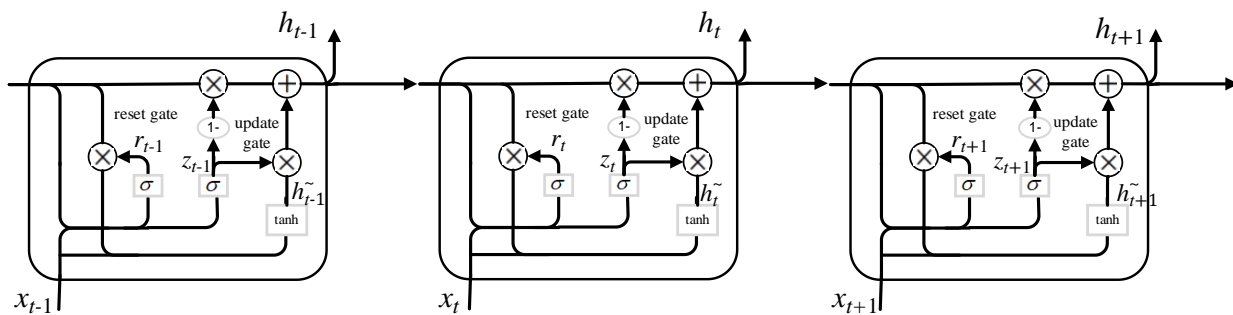


Fig. 3 – GRU network structure

As shown in Fig. 3, x_{t-1} , x_t and x_{t+1} represent the input of the previous moment, the current moment, and the next moment, respectively, h_{t-1} , h_t and h_{t+1} represent the hidden state of the previous node, the current node, and the next node, respectively, h_{t-1}^{\sim} , h_t^{\sim} and h_{t+1}^{\sim} represent the candidate hidden states, r_t and z_t represent the reset gating and update gating, respectively, and σ represents the activation sigmoid function.

The states of the reset gate and update gate at time t are defined as:

$$\begin{cases} r_t = \sigma(w_r x_t + u_r h_{t-1}) \\ z_t = \sigma(w_z x_t + u_z h_{t-1}) \end{cases} \quad (7)$$

where w_r , u_r , w_z and u_z represent the weight matrixes.

The hidden state h_t and the candidate hidden state \tilde{h}_t at time t are defined as:

$$\begin{cases} h_t = (1 - z_t)h_{t-1} + z_t\tilde{h}_t \\ \tilde{h}_t = \tanh(w_h x_t + u_t(r_t \cdot h_{t-1})) \end{cases} \quad (8)$$

where

$$\begin{cases} \sigma(x) = \frac{1}{1 + \exp(-x)} \\ \tanh(x) = \frac{1 - \exp(-2x)}{1 + \exp(-2x)} \end{cases} \quad (9)$$

In the output layer:

$$y_t = h_t \cdot w \quad (10)$$

where w is the weight matrix of the output layer.

The training process of the GRU model is as follows:

- (1) Learning weight matrix parameters by the forward propagation.
- (2) Calculate the sample loss in the transmission by the forward network.
- (3) Learn network update parameters by the backward error propagation.

The GRU model's parameters in this research are shown in Table 4.

Table 4

| GRU model's parameters | |
|---------------------------------------|---------------------------------------|
| Parameters | Parameter value |
| Training set | 70% of all data sets |
| Test set | 30% of all data sets |
| Optimizer | SGD random gradient descent optimizer |
| Momentum parameter | 0.8 |
| Learning rate attenuation | 10^{-5} |
| Regularization of random deactivation | 0.1 |
| Hide layer activation function | Sigmoid() |
| Input dimension | 3 |
| Number of Network layer | 30 |
| Output layer activation function | tanh() |
| Learning rate | 0.001 |

• **EEMD-GRU model**

The empirical mode decomposition (EMD) method can decompose a signal into several IMFs and one RES that reflects the overall trend of the signal based on the local characteristics of the original signal. EMD method does not need to select any function as the base, and has the adaptive capability, which is suitable for the data processing of non-linear and non-stationary signals. The decomposition formula is given by

$$x(t) = \sum_{i=1}^n c_i(t) + r_n(t) \quad (11)$$

where c_1, c_2, \dots, c_n represent the IMFs obtained by the decomposition of the original signal $x(t)$, with each IMF containing a single time scale, and $r_n(t)$ represents the residue (RES).

The ensemble empirical mode decomposition (EEMD) is an improvement to the EMD method, which overcomes the phenomenon of modal aliasing in the EMD method. If there is a sudden change in the time scale of a signal, there will be an IMF component containing different time scales. By adding white noise to the original signal sequence, EEMD performs smoothing processing on the abrupt changes in the time scale, and uses the uniform distribution of white noise spectrum to make the signals of different scales adaptively map to the appropriate reference scale. At the same time, by adding white noise multiple times to perform EMD and obtain the average result, the influence of noise is eliminated. Finally, the IMF component containing a single time scale is obtained. The decomposition steps of EEMD are as follows (Chen R., 2012):

- (1) Add M Gaussian white noise $n_i(t)$ ($i = 1 \sim M$) with an amplitude of 0 and constant amplitude standard deviation to the original signal $x(t)$ to obtain $x_i(t)$, as shown below.

$$x_i(t) = x(t) + n_i(t) \quad (12)$$

(2) Perform EMD on $x_i(t)$ respectively to obtain the IMFs and RES, and record the j th IMF as $c_{ij}(t)$ and the RES as $r_i(t)$.

(3) Perform average calculation on the IMFs, and obtain the final result of EEMD, as shown below.

$$c_j(t) = \frac{1}{M} \sum_{i=1}^n c_{ij}(t) \tag{13}$$

The flow chart of EEMD is shown in Fig. 4.

By performing EEMD on the time series data of ammonia concentration in the broiler house, the ammonia concentration series are decomposed into 8 IMF components and 1 RES component, which achieves the separate processing for different characteristic components, thereby improving the prediction accuracy. Then, the GRU model is established for each component, and finally, the prediction results of the components are summed to obtain the final prediction result. The flow chart of the EEMD-GRU model is shown in Fig. 5.

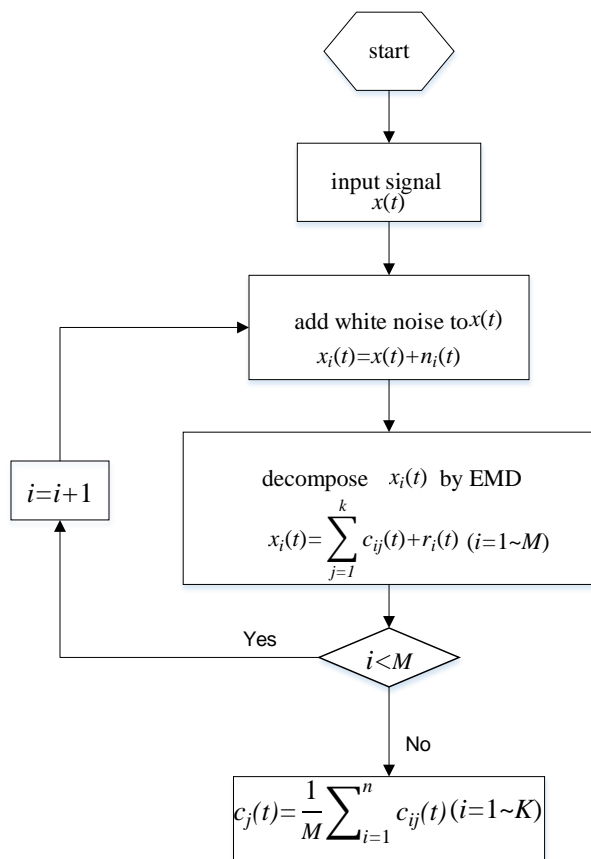


Fig. 4 – Flow chart of EEMD model

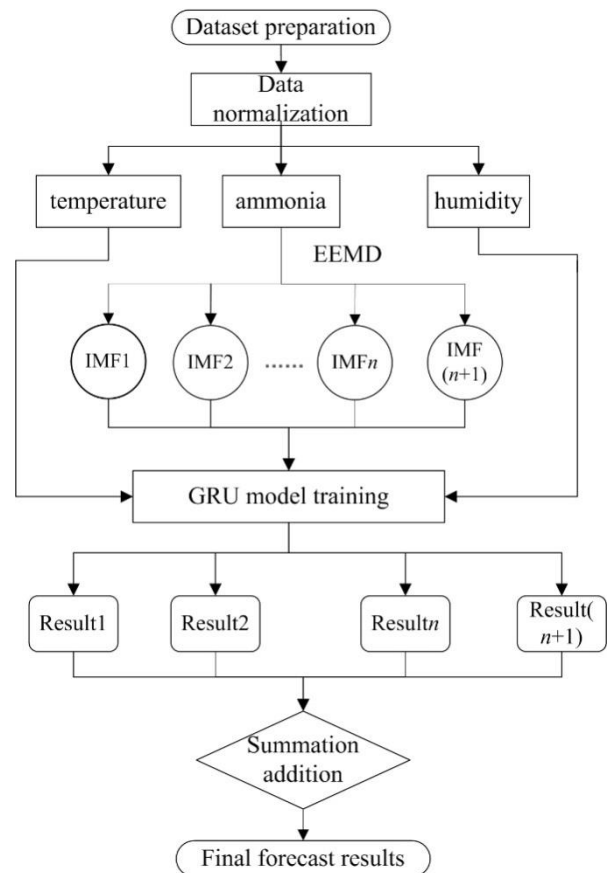


Fig. 5 - Flow chart of EEMD-GRU model

RESULTS AND DISCUSSION

Data Trends

Based on the data set used in the experiment, the trend of the environmental data in the broiler house is obtained, as shown in Fig. 6.

It can be seen from Fig. 6 that the temperature inside and outside the broiler house was maintained at about 15°C during the experimental period from December 5 to January 12. After 16 days from the start of the experiment (December 21), the temperature inside and outside the broiler house gradually decreased and fluctuated around 10°C. It can be seen from the figure that the humidity of the broiler house changed greatly during a whole day, with higher humidity at night, and lower humidity in the daytime.

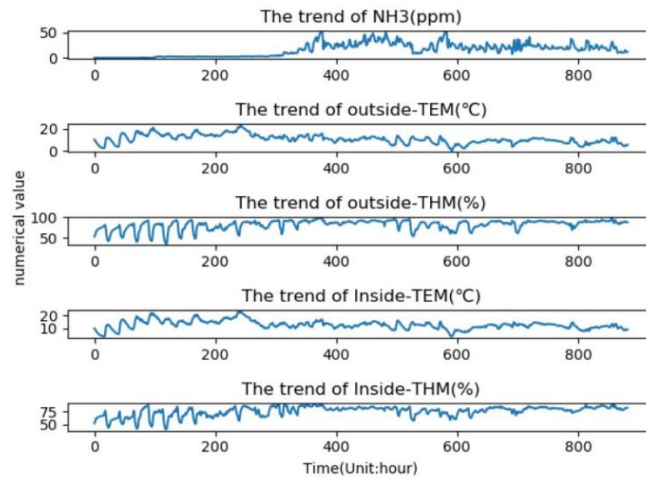


Fig. 6 - Trend of the environmental data

The highest relative humidity is about 90% and the lowest is about 40%. The temperature and humidity inside and outside the broiler house had the same change trend. For the trend of ammonia concentration, it can be clearly seen that the change in the ammonia concentration underwent a cumulative process. At the beginning of the experiment, there was no ammonia in the house and the ammonia concentration is 0. As the experiment went on, ammonia gas was generated, and the concentration continued to increase with the increase of the experimental time. The ammonia concentration reached the maximum value of 50 ppm at about 15 days after the broilers entered the chicken house. In order to protect the health of the broiler, the ventilation system started to regulate the ammonia concentration. It can be seen that the ventilation system had well controlled the ammonia concentration in the broiler house.

EEMD Results

The ammonia concentration data in the broiler house has obvious non-linear and unstable characteristics. In this paper, the EEMD algorithm is performed on the ammonia concentration data collected in 38 days, from December 5, 2019 to January 12, 2020. The ammonia concentration data in the broiler house is used as the input and the components and residuals of the ammonia concentration data are used as the output, as shown in Fig. 7.

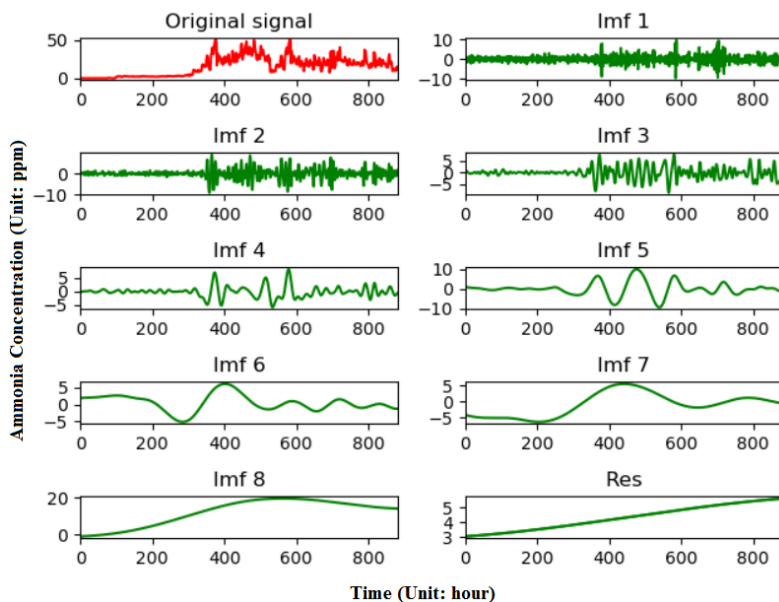


Fig. 7 - Decomposition results of EEMD algorithm

It can be seen from the decomposition results in Fig. 7 that the EEMD algorithm decomposes the ammonia concentration data into 8 IMF components and 1 RES component. Specifically, the IMF1-IMF3 components have a high frequency and have a certain random disorder, which reflects the influence of random uncertain factors inside and outside the house on the characteristics of the ammonia concentration

in the house. As the decomposition goes on, the volatility and frequency of the IMF component decrease in order. The RES component is a low-frequency component, which reflects the overall change trend of the original ammonia concentration data during the experiment. The original data sequence can be obtained by adding each component.

Prediction Results

In this research, the ammonia concentration is predicted according to the parameters of the BP model, GRU model, and EEMD-GRU model. A comparison is conducted on the prediction results of the three models. The prediction results are shown in Fig. 8, Fig. 9, and Fig.10.

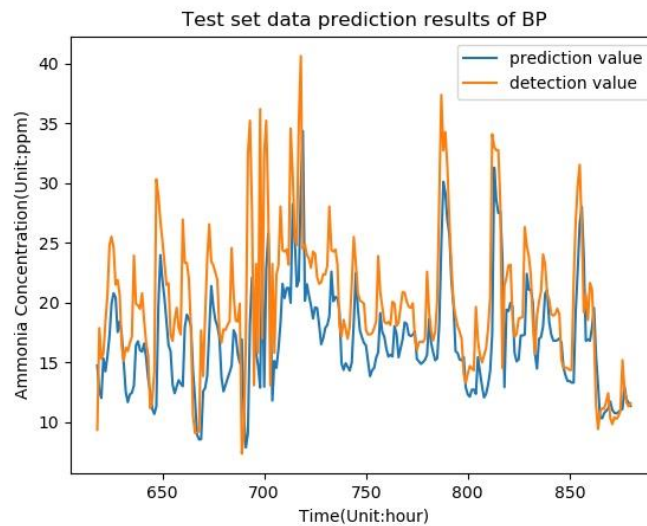


Fig. 8 - Prediction result curve of the BP model

From Fig. 8, it can be seen that the ammonia concentration fluctuates greatly during the experiment, showing strong instability and fluctuation. The prediction result of the BP model is roughly consistent with the true curve. However, it can also be observed that the prediction result curve by the BP model is slightly lagged behind the true curve, and the difference between the two is larger on the vertical axis, especially in the range of 630 h to 670 h and 725 h to 800 h. The maximum difference reaches about 20 ppm. In the final prediction result, Test RMSE is 6.2 ppm and Test MAE is 4.9 ppm.

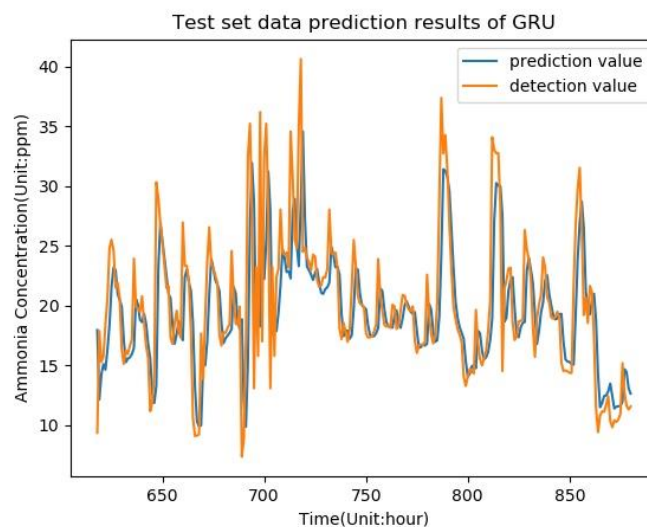


Fig. 9 - Prediction result curve of the GRU model

From Fig. 9, it can be seen that the prediction result curve of the GRU model is more consistent with the true curve than the BP model. The problem of lag in the two curves disappears, and the error is reduced. Especially in the range of 680 h to 710 h and at the time of about 850 h, the two curves can basically

coincide. The curves from 630 h to 670 h and 725 h to 800 h are also close, better than the result by the BP model. However, it can be seen that the maximum error is still around 17 ppm, and the prediction accuracy needs to be further improved. In the final prediction result, Test RMSE is 4.4 ppm and Test MAE is 2.8 ppm.

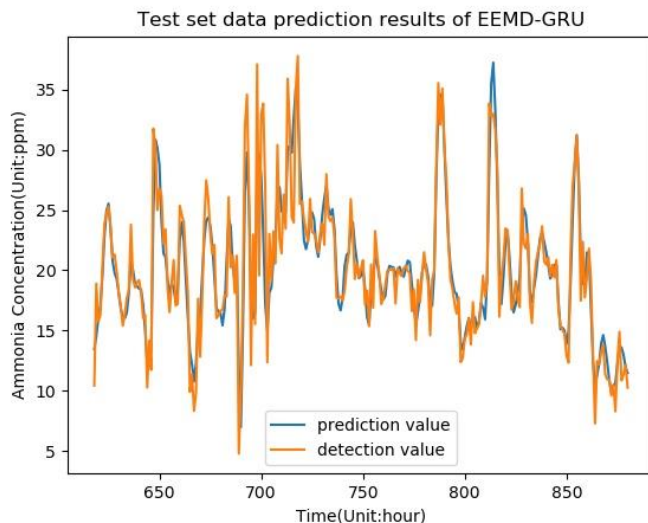


Fig. 10 - Prediction result curve of the EEMD-GRU model

From Fig. 10, it can be clearly seen that the prediction result using the EEMD-GRU model are more accurate than the previous two models. The two curves can basically coincide at more points in time, and the maximum error is also reduced to about 4 ppm. In the final prediction result, Test RMSE is 2.4 ppm and Test MAE is 1.6 ppm. From the perspectives of both intuitive judgment and the final error, the EEMD-GRU model has fewer errors and better accuracy than the BP model and GRU model.

Table 5 shows the comparison of the prediction errors of the three models.

Table 5

Comparison of the prediction errors of the three models

| Model | Root mean square error(ppm) | Mean absolute error(ppm) |
|----------|-----------------------------|--------------------------|
| BP | 6.2 | 4.9 |
| GRU | 4.4 | 2.8 |
| EEMD-GRU | 2.4 | 1.6 |

CONCLUSIONS

In this paper, the EEMD-GRU model has been used to predict the ammonia concentration in a broiler house for yellow-feather broilers. The experimental data of the broiler house from December 5, 2019 to January 12, 2020 were used as the data set. The generation of ammonia concentration has a strong correlation with the age of broilers entering the house. When the number of broilers in the house was 45, the ammonia concentration reached the highest concentration 15 days after the broilers entered the house. After that, the ammonia concentration decreased through the ventilation control system. The first 70% of the data set was used as the training set, and 30% was used as the test set. After 1000 iterations of the model, the prediction results were obtained. For the EEMD-GRU model results, the root mean square error is 2.4 ppm, and the mean average error is 1.6 ppm, which are higher than 6.2 ppm and 4.4 ppm of the BP mode and 4.9 ppm and 2.8 ppm of the GRU model. The EEMD-GRU model has shown the highest accuracy.

The EEMD-GRU model proposed in this paper can decompose the data with large volatility and non-stationarity to obtain relatively stable data, which effectively improves the prediction accuracy. The accurate and timely prediction of the ammonia concentration data in the broiler house will help breeders make accurate judgments on the environment of broiler houses, effectively reduce the damage of harmful gases to broilers, and improve the yield and quality.

ACKNOWLEDGEMENT

This research was jointly supported by the Fundamental Research Funds for the Central Universities of China (KYTZ201661), China Postdoctoral Science Foundation (2015M571782).

REFERENCES

- [1] Chen R., Tang B. and Ma J., (2012), Adaptive de-noising method based on ensemble empirical mode decomposition for vibration signal, *Journal of Vibration and Shock*, Vol. 31, Issue 15, pp. 82-86, London/England;
- [2] Guo M., Wang P. and Zhao L., (2019), Research on recognition method of transportation modes based on deep learning, *Journal of Harbin Institute of Technology*, Vol. 51, Issue 11, pp. 1-7, Haerbin/China;
- [3] Hao G., (2019), Research and implementation on air quality prediction method deep learning based, Beijing University of Posts and Telecommunications, Beijing/China;
- [4] Hu M., Lu W., Xu C., et al., (2019), Satellite RCS anomaly detection using the GRU model, *Journal of Xidian University*, Vol. 46, Issue 06, pp. 125-130, Xian/China;
- [5] Huo C., (2018), Research of remote monitoring system of piggery environment based on LoRa and prediction model of ammonia concentration, *Jiangsu university*, Zhenjiang/China;
- [6] Liu W., Han H., Gao J., et al., (2019), Study on distribution rule of atmospheric ammonia in standardized broiler house, *Shandong Agricultural Sciences*, Vol. 51, Issue 08, pp. 79-83, Jinan/China;
- [7] Majd M. and Safabakhsh R., (2019), Correlational convolutional LSTM for human action recognition, *Neurocomputing*, Available online 24 April, <https://doi.org/10.1016/j.neucom.2018.10.095>, Amsterdam/Netherlands;
- [8] Muzaffar S. and Afshari A., (2019), Short-term load forecasts using LSTM networks, *Energy Procedia*, Vol. 158, pp. 2922-2927, Hongkong/China;
- [9] Pu M. and Ge Y., (2019), Attention based GRU network for domain adaptation in sentiment classification, *International Conference on Computation and Information Sciences*, Chengdu/China;
- [10] Ribeiro R., Casanova D., Teixeira M., et al., (2019), Generating action plans for poultry management using artificial neural networks, *Computers and Electronics in Agriculture*, Vol. 161, pp. 131-140, Oxford/England;
- [11] Shen D., Dai P., Wu S., et al., (2018), Distribution of particles, ammonia and carbon dioxide as well as physicochemical property of pm2.5 in an enclosed broiler breeder house in winter, *Chinese Journal of Animal and Veterinary Sciences*, Vol. 49, Issue 06, pp. 1178-1193, Beijing/China;
- [12] Xie Q., (2015), Environmental suitability assessment and control model development for a swine house based on fuzzy theory, *Northeast Agricultural University*, Haerbin/China;
- [13] Xu W., Zhang L. and Gu X., (2011), Soft sensor for ammonia concentration at the ammonia converter outlet based on an improved particle swarm optimization and BP neural network, *Chemical Engineering Research and Design*, Vol. 89, Issue 10, pp. 2102-2109, Rugby/England;
- [14] Yao H., Sun Q., Zou X., et al., (2018), Research of yellow-feather chicken breeding model based on small chicken chamber, *INMATEH - Agricultural Engineering*, Vol. 56, Issue 3, pp. 91-100, Bucharest/Romania;
- [15] Yao Z., (2008), Effects of different ammonia concentrations on growth, immunity and physiological-biochemical parameters in broiler chickens, *Zhejiang University*, Hangzhou/China;
- [16] Zhang J., Wang X., Zhao C., et al., (2019), Application of cost-sensitive LSTM in water level prediction for nuclear reactor pressurizer, *Nuclear Engineering and Technology*, Available online 27 December, <https://doi.org/10.1016/j.net.2019.12.025>, Daejeon/South Korea;
- [17] Zhang S., Ding A., Zou X., et al., (2019), Simulation analysis of a ventilation system in a smart broiler chamber based on computational fluid dynamics, *Atmosphere*, Vol. 10, Issue 6, no. 315, Basel/Switzerland;
- [18] Zhang X., Ding A., Zou X., et al., (2019), Prediction of ambient temperature in the chambers for yellow feather chickens based on least squares support vector machine optimized by improved particle swarm optimization algorithm. *International Agricultural Engineering Journal*, Vol. 28, Issue 4, no. 9, Beijing/China;
- [19] Zilio M., Orzi V., Chiodini M., et al., (2020), Evaluation of ammonia and odour emissions from animal slurry and digestate storage in the Po Valley (Italy), *Waste Management*, Vol. 103, pp. 296-304, Oxford/England.